

1 **On-line breath gas analysis in unrestrained mice by hs-PTR-MS**

2

3 Wilfried Szymczak¹, Jan Rozman^{2,3}, Vera Höllriegl¹, Martin Kistler², Stefan Keller¹, Dominika Peters^{1,2},
4 Moritz Kneipp¹, Holger Schulz⁴, Christoph Hoeschen¹, Martin Klingenspor³ and Martin Hrabě de
5 Angelis²

6 ¹ Helmholtz Zentrum München - German Research Center for Environmental Health (GmbH), Research
7 Unit Medical Radiation Physics and Diagnostics, 85758 Neuherberg, Germany

8 ² Helmholtz Zentrum München - German Research Center for Environmental Health (GmbH), Institute of
9 Experimental Genetics, German Mouse Clinic, 85758 Neuherberg, Germany

10 ³ ZIEL Department of Molecular Nutritional Medicine, Else Kröner-Fresenius Center, Technische
11 Universität München, 85350 Freising, Germany

12 ⁴ Helmholtz Zentrum München - German Research Center for Environmental Health (GmbH), Institute of
13 Epidemiology I, 85758 Neuherberg, Germany

14

15 Corresponding author: Wilfried Szymczak

16 Email: Szymczak@helmholtz-muenchen.de

17 Phone: +49 89 3187 2949

18 Fax: +49 89 3187 2517

19

20 **Abstract**

21 The phenotyping of genetic mouse models for human disorders may greatly benefit from breath gas
22 analysis as a noninvasive tool to identify metabolic alterations in mice. Phenotyping screens such as the
23 German Mouse Clinic demand investigations in unrestrained mice. Therefore, we adapted a breath screen
24 in which exhaled volatile organic compounds (VOCs) were online monitored by proton transfer reaction
25 mass spectrometry (hs-PTR-MS). The source strength of VOCs was derived from the dynamics in the
26 accumulation profile of exhaled VOCs of a single mouse in a respirometry chamber. A careful survey of
27 the accumulation revealed alterations in the source strength due to confounders, e.g., urine and feces.
28 Moreover changes in the source strength of humidity were triggered by changes in locomotor behavior
29 $a_{S_{\text{Mice}}}$ showed a typical behavioral pattern from activity to settling down in the course of subsequent
30 accumulation profiles. We demonstrated that metabolic changes caused by a dietary intervention, e.g.,
31 after feeding a high-fat diet (HFD) a sample of 14 male mice, still resulted in a statistically significant
32 shift in the source strength of exhaled VOCs. Applying a normalization which was derived from the
33 distribution of the source strength of humidity and accounted for varying locomotor behaviors improved
34 the shift. Hence, breath gas analysis may provide a noninvasive, fast access to monitor the metabolic
35 adaptation of a mouse to alterations in energy balance due to overfeeding or fasting and dietary
36 macronutrient composition as well as a high potential for systemic phenotyping of mouse mutants,
37 intervention studies, and drug testing in mice.

38 **Introduction**

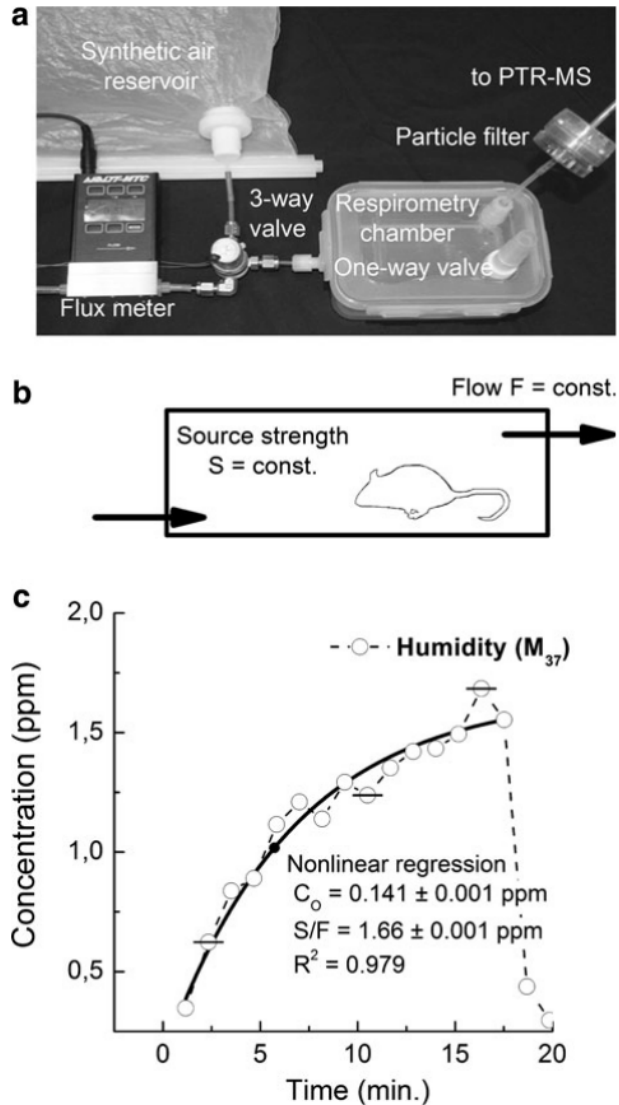
39 Numerous endogenous volatile organic compounds (VOCs) are exhaled while breathing. VOCs mainly
40 originate from metabolic processes in cells and are distributed via the circulating blood; they pass the
41 alveolar-capillary membrane, enter the volume of the lungs, and are finally exhaled. The composition and
42 abundance of VOCs in breath gas can be used to draw conclusions about metabolic status and specific
43 physiological processes. The analysis of VOCs in exhaled breath gas samples has already been used in
44 studies on human disorders (Whittle et al. 2007), such as cancer (Bajtarevic et al. 2009; Phillips et al.
45 1999a) or on healthy humans (Smith et al. 2007). By means of gas chromatography and mass
46 spectrometry, a total of about 3500 VOCs was identified in a study comprising 50 healthy humans
47 (Phillips et al. 1999b). Notably, in single subjects of the study, an average number of only about 200
48 substances could be detected, 27 of which were ubiquitously found in all participants. This distribution
49 suggested (a) that there is a considerable inter-individual variability and (b) that this variability could
50 provide a high diagnostic potential for the analysis of shifts in VOC abundance to draw conclusions about
51 the attributed specific metabolic processes. State-of-the-art breath gas analysis (Cao and Duan 2007) in

52 humans is based on mass spectrometry in combination with preselection or selective ionization (e.g., gas
53 chromatography mass spectrometry (Miekisch et al. 2004), selected ion flow tube mass spectrometry
54 (Smith et al. 2007), ion mobility spectrometry (Vautz et al. 2010), and proton transfer reaction mass
55 spectrometry (PTR-MS) (Hansel et al. 1998; Lindinger et al. 1998)). Breath gas analysis was only rarely
56 applied in small rodents. As early as in 1974, Riely and Cohen reported on the ethane evolution in mice
57 stimulated and diminished by prior injection of drugs (Riely et al. 1974). Further analyses were also
58 restricted to single VOCs, such as ethanol (Cope et al. 2000), ethane (Risby et al. 1999), or $^{13}\text{CO}_2$
59 (Friedrich et al. 2011; Isken et al. 2010). A range of VOCs in the breath of intubated spontaneously
60 breathing mice during anesthesia was provided by ion mobility spectrometry coupled with a
61 multicapillary column (Vautz et al. 2010). Very recently Aprea et al. reported on a fast online method
62 with a nose tube for collection and analysis of exhaled breath in a single rat by PTR-TOF-MS (Aprea et
63 al. 2012). PTR-MS measures a wide spectrum of VOCs online, fast and almost simultaneously over a
64 range of concentrations from ppm (part-per-million) down to ppt (part-per-trillion) levels (Hansel et al.
65 1998). To our knowledge, the implementation of this method in studies including animal models, such as
66 the laboratory mouse, is not applied even though this species is widely used in biomedical and genome
67 research (Hrabe' de Angelis and Strievens 2001). Due to the recent technological progress in PTR-MS,
68 the standardized investigation of exhaled VOCs of unrestrained, small animals, such as a_{Mice} has the
69 potential to provide large data sets for metabolic profiling. These data contribute to the characterization of
70 the specific metabolic state of individual mice during screening procedures, for example, in
71 comprehensive phenotyping centers for mouse mutants such as the German Mouse Clinic (GMC) (Fuchs
72 et al. 2009). Phenotyping of genetic mouse models for human disorders had been identified as area of
73 highest relevance in genome and biomedical research. Therefore, the aim of our study was to develop a
74 PTR-MS setup suitable for unrestrained screening of exhaled VOCs in mouse models of human diseases.
75 The major challenges of the method described here were to adapt the PTR-MS sampling of breath gas to
76 the dimensions of a mouse, to sort out VOCs that are due to contaminations (urine, feces, food, etc.)
77 confounding the analysis, to identify VOCs that are mainly due to exhaled breath of mice, and to develop
78 a data analysis procedure that is suitable to be integrated into a high-throughput phenotyping screen. In
79 this article, we describe a basic setup—consisting of a respirometry chamber and breath gas analysis
80 (PTR-MS)—to implement this noninvasive and very sensitive online method in the workflow of the
81 energy metabolism module of the GMC.

82 **Methods**

83 **Measuring setup**

84 The basic measuring setup is depicted in Fig. 1a. The respirometry chamber consisted of a transparent
85 polypropylene box (volume: 600 ml). A large top cover opened up easily so that the mouse could be
86 transferred easily into and out of the box. The respirometry chamber was connected to the PTR-MS (air
87 flow 90 ml min^{-1}) and face-to-face to a Teflon bag reservoir (capacity of 10 l, Welch Fluorocarbon Inc.,
88 Dover, USA) filled with VOC free, synthetic air (20 % oxygen, 80 % nitrogen, concentration of
89 hydrocarbons B0.1 ppm, Linde AG, Germany). The tube feed-throughs were made of polypropylene and
90 all connecting tubes were made of Teflon and a PFTE membrane filter (pore size 2.0 μm , PALL
91 Corporation, Ann Arbor, USA) cleaned the air stream into the heated inlet capillary of the PTR-MS from
92 particular contaminations. Alternatively, a 3-way valve opened the ventilation path (flow 2.5 l min^{-1} ,
93 volume 6 l). Keeping the disturbance of a mouse in the box as small as possible, the jet of synthetic air
94 into the box was deflected through a simple baffle fixed at the outlet of the feed-through used for the
95 ventilation. A one-way mouthpiece (ENVITEC-WISMAR GmbH, Wismar, Germany) mounted on the
96 top cover opened during ventilation to prevent an overpressure in the box. The leak-proof nature of the
97 feed-throughs and of the top cover was carefully and routinely controlled (blank profile). The inlet
98 capillary and the drift tube of the PTR-MS were kept constant at $60 \text{ }^\circ\text{C}$, whereas the respirometry chamber
99 was in equilibrium with ambient temperature comparable to home cage conditions. The repeated flushing
100 of the chamber and continuous diluting of the headspace in presence of a mouse kept the temperature
101 within the chamber at ambient temperature ($24 \pm 2 \text{ }^\circ\text{C}$). To control the conditions in the respirometry
102 chamber inducing for hypercapnea, we determined typical CO_2 concentrations during a VOC
103 measurement using a portable carbon dioxide analyzer (CA-10, Sable Systems International Inc, Las
104 Vegas, NV, USA). When adjusted to the air flow of 90 ml min^{-1} into the PTR-MS, the concentration of
105 CO_2 was $\leq 3 \text{ vol}\%$ at the end of the accumulation period, i.e., 20 min after the flushing.



106

107 **Fig. 1** a Basic respirometry setup. The respirometry chamber (volume: 600 ml) is connected to the PTR-
 108 Quad-MS (flow 90 ml min^{-1}) and face-to-face to a bag reservoir filled with VOC free, synthetic air. The
 109 Teflon filter cleans the air stream into the PTR-MS from particular contaminations. Alternatively, the
 110 three-way valve opens the ventilation path (flow 2.5 l min^{-1} , volume 6 l). b Description of the dynamic
 111 changes in the respirometry chamber by a simple chamber model. The compartment model assumes that a
 112 mouse exhales a compound of mass M with a constant source strength S into a head space volume of 600
 113 ml. The constant flow of gas F through the chamber dilutes the concentration of this compound. The gas
 114 reservoir connected to the chamber maintains equilibrium in pressure. c Accumulation profile of humidity
 115 recorded in the respirometry chamber and fitting of the profile with the solution function of the chamber
 116 model. The nonlinear regression fit of the solution function of the model equation to a measured profile of
 117 humidity determines the values of the two free parameters, the concentration at $T = 0$, C_0 and the ratio S/F

119 **PTR-MS**

120 In the development of the basic set-up and the pilot nutrition study, a high-sensitivity proton transfer
121 reaction mass spectrometer (hs-PTR-Quad-MS; Ionicon Analytic GmbH, Innsbruck, Austria) was used.
122 Details of the measuring principle and applications have previously been reported in detail (Lindinger et
123 al. 1998). In brief, the breath sample is injected into a drift tube together with a beam of hydronium ions.
124 VOCs with a proton affinity higher than that of the hydronium ion are ionized by the proton transfer
125 reaction. According to the selective ionization, VOCs can be measured with concentrations ranging from
126 ppm down to the ppt level in the presence of high concentration of the main components of exhaled
127 breath (e.g., nitrogen, oxygen, humidity, and carbon dioxide). As a result of the proton transfer reaction,
128 all the mass numbers refer to protonated mass numbers. The PTR-MS was operating with a count rate of
129 the primary ions (H_3O^+) of $\approx 2.0 \cdot 10^7 \text{ counts} \cdot \text{s}^{-1}$, and the percentage of the minor precursor ion O_2^+ was
130 kept below 1 % of the count rate of the primaries. The pressure in the drift tube was $\approx 2.2 \text{ mbar}$. The drift
131 tube and all connecting tubes from the respirometry chamber to the drift tube inlet were kept at a
132 temperature of $60 \text{ }^\circ\text{C}$ for preventing condensation of the humidity. The measured raw count rate of a
133 signal at mass M_i , $\text{cps}(M_i)$ was normalized to the count rate of the precursor ion and the water cluster at
134 M_{37} according to (Hansel et al. 1998), denoted as n_{cps} . Other water clusters were neglected because the
135 count rate was at least two orders of magnitude smaller than that of the first water cluster (e.g.,
136 $\text{cps}(M_{55})/\text{cps}(M_{37}) \leq 0.003$). The PTR-MS instrument was calibrated with standard $\text{gas}_{\text{mixtures}}$ with a
137 specified concentration of $100 \pm 10 \text{ ppb}$ for each compound (Aromatic subset mix, Scott Speciality Gases,
138 Plumsteadville, USA). A daily control of the optimum saturation voltage the SEM was done to detect
139 changes in the sensitivity. For the calculation of the volume ratio (e.g., in part per billion, ppb) for a single
140 compound, the standard formula for PTR-MS concentrations was used (Hansel et al. 1998). The relative
141 uncertainty in the derived concentration in ppb due to the uncertainty in the measured count rate estimated
142 to 10 % or less along within an accumulation measurement. The PTR-MS recorded full mass spectra in
143 the mass range from $m/z = 21$ to 160. With a chosen dwell time of 500 ms, a full mass scan took 70 s.
144 Therefore, a time series of mass scans recorded one-by-one built up a VOC profile. The used PTR-MS
145 was equipped with a quadrupole mass separator tuned to unit mass resolution. The assignment of a
146 compound to mass was in most cases tentatively especially at higher masses. The assignment of methanol
147 to M_{33} was beyond question, and the assignment of M_{59} to acetone was highly supported by the correlation
148 between the count rates of the two acetone isotopes at M_{59} and M_{60} . In the PTR-Quad-MS measurements,
149 the adjoined masses of CO_2 and acetaldehyde were not resolved. In this feasibility study, the validation by
150 GC-MS was not yet available because of the complex mixture in presence of humidity. The monitoring

151 of the repeatability of exhaled VOCs in separate samples of male C57BL/6J mice were done using a
152 PTR-TOF2000-MS (Ionicon Analytic GmbH, Innsbruck, Austria), which was equipped with a drift-tube
153 common in the hs-PTR-MS. The TOF mass-analyzer principle has been described elsewhere (Jordan et al.
154 2009).

155 **Hierarchical cluster analysis**

156 Standard hierarchical cluster analysis (HCA) was carried out using the hclust function in the Stats
157 Package of the statistical computing program R (<http://www.R-project.org>). Input variables (e.g., times
158 series of the concentration of $mas_{S_{Mi}}$) were scaled to the mean and standard deviation of the time series,
159 and the complete agglomeration method was applied. The scaling of the variables to a mean rather than to
160 the median of the time series was supported by the finding that in the former case, the undisturbed
161 isotopes of a compound were represented by a forklike subcluster. Noisy mass variables were excluded
162 from the input matrix of variables. As a rule, all masses, normalized count rates of which fall below a
163 threshold value of 2 ncps for at least half of the values in a time series, were excluded.

164 **Mice housing and nutrition**

165 For the diet intervention study, 12-week-old male C57BL/6N mice were ordered from Charles River
166 Laboratories (Sulzfeld, Germany). The study on repeatability of VOC accumulation profiles was
167 conducted in 8–22-week-old male C57BL/6J mice from the in-house breeding stock. Upon arrival, mice
168 were housed in individually ventilated cages (Ventirack, Biozone, UK) at the GMC. The animal
169 experiments were approved by the Government of the Federal State of Bavaria, Germany. The animal
170 facility was tested for microorganisms according to the FELASA recommendations for mouse health
171 monitoring (Nicklas et al. 2002). Husbandry conditions were as follows: room temperature 20–24 °C, air
172 humidity 50–60 %, 20 air changes per hour, and light regimen on a 12 h light/dark cycle. Wood shavings
173 (Altromin GmbH, Germany) were applied as bedding material. Mice had access to drinking water and
174 food ad libitum. The mice were fed with a standard lab chow (no. 1314, Altromin, Lage, Germany). For
175 the high-fat diet (HFD) challenge, mice were fed a purified experimental diet containing 60 energy% of
176 fat (E 15741-347, Ssniff, Soest Germany). Mice were weighed in the morning once every week and at the
177 day of the VOC analysis. VOCs in mouse breath gas were monitored immediately before the diet
178 intervention and three weeks after feeding the HFD during daytime. To minimize daily variation in VOC
179 concentrations, mice were measured exactly in the same order and at the same time of the day as in the
180 initial trial.

181 **Minute volume of breath of mice**

182 The minute volume of mice was measured in a whole body plethysmograph (Buxco Electronics, Sharon,
183 Connecticut, USA) according to the principle described by Drorbaugh and Fenn (1955). Through
184 calibration, the pressure swings arising from inspiration and expiration of the mouse are transferred in
185 flow and volume signals. Automated data analysis provides tidal volumes, respiratory rates, and minute
186 ventilation at 10-s intervals. During the measurements, the air in the chamber volume (600 ml) was
187 diluted with clean air at a flow rate of 200 ml min⁻¹. A flushing of the plethysmograph for 2 min at a rate
188 of 3 l min⁻¹ minimized the concentration of the VOCs before a profile was recorded. At the same time, the
189 PTR-MS was connected to the chamber, and a constant flow of 47 ml min⁻¹ was bypassed to the PTR-MS.
190 To match the time resolution of the pressure measurement, the PTR-Quad-MS recorded only 10 masses
191 with a high count rate in the multiple ion mode with reduced dwell times.

192 **Results**

193 To develop a robust and efficient but also specific and highly automated phenotyping method for mice
194 based on breath gas analysis poses challenges in many respects. Our solution rested upon the
195 accumulation of breath exhaled of a single mouse kept in a clean respiratory chamber to overcome the
196 limitation of minute volume of breath in an online analysis set-up. Accumulation profiles disturbed by
197 confounders from urine and feces were discarded. VOCs in the head space predominantly originating
198 from exhaled breath were described by the dynamic change during the accumulation, i.e., the source
199 strength. Activity levels clearly affect breathing frequency as well as the exhaled minute volume. The
200 adaption to the breath gas analysis device (hs-PTR-MS) and the basics of the strategy are described
201 below.

202 **Accumulation profiles of exhaled VOCs**

203 The disposable gas volume of a single breath of a mouse [tidal volume 0.2–0.3 ml (Reinhard et al. 2002)]
204 was out of scope to be analyzed by PTR-MS. Therefore, the accumulation of exhaled VOCs was
205 monitored within the defined volume of a clean small respirometry chamber and after controlled
206 ventilation with clean air. After placing a mouse into the respirometry chamber, a tenfold ventilation of
207 the volume of the respirometry chamber with synthetic air resets the humidity as well as the concentration
208 of all VOCs to a low basal level. Then, the accumulation of VOCs was monitored for 20 min by recording
209 mass spectra one by one. As an example, the signal for humidity at $m/z = 37$ (M 37) showed an up to
210 sixfold increase from initially very low levels (Fig. 1c). The signal of M₃₇ in an empty respiratory chamber
211 increased only twofold to roughly 10 % of the level of M₃₇ in the presence of a mouse.

212 **Determination of the source strength of exhaled VOCs**

213 The quantification of the exhaled concentration of VOCs using the difference between end and starting
214 levels requires the careful monitoring of basal and saturation values. Keeping the residence time of a
215 mouse in the respirometry chamber short resulted in accumulated concentrations which generally were
216 below saturation. Therefore, our quantification scheme was based on the dynamic changes during the
217 accumulation. With the help of a respirometry chamber model (Fig. 1b), the source strength S of an
218 exhaled VOC, given in ppb ml min^{-1} , was determined. In a first approach, we described the concentration
219 of a VOC C_i at time t through a constant source strength S_i which is counterbalanced by the steady flow
220 rate F out of the respirometry chamber.

$$221 \quad (1) \frac{dC_i(t)}{dt} = \frac{1}{V} (S_i - C_i(t) \times F)$$

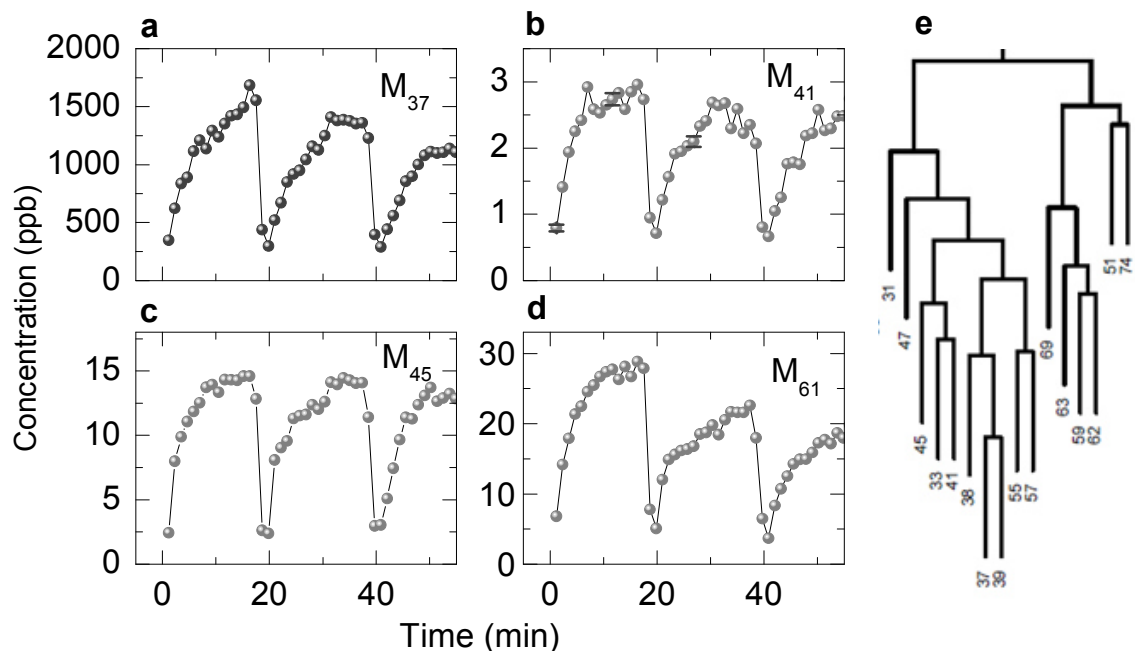
222 The solution of the equation (1)

$$223 \quad (2) C_i(t) = C_0 \times e^{-\frac{F}{V}t} + \frac{S_i}{F} \left(1 - e^{-\frac{F}{V}t}\right)$$

224 includes two free parameters, C_0 and S_i/F . C_0 , which is the basal concentration after the ventilation, can be
225 experimentally kept small by sufficiently flushing the respirometry chamber with clean synthetic air.
226 Because F was constant, S_i can be calculated from the second free parameter. A nonlinear least-square
227 fitting was applied to the monitored profiles between two ventilations (Fig. 1c). When applied to the
228 undisturbed humidity profiles, the solution of the respirometry chamber model described the profiles
229 sufficiently well (e.g., for humidity $R^2 = 0.979$), suggesting that it was possible to calculate the source
230 strength from the respirometry chamber model as a main factor reflecting the concentrations of specific
231 VOCs in the exhaled breath.

232 **Identifying VOCs originating from breath**

233 Every breath of a mouse replaced a small volume of dry air in the respirometry chamber with saturated
234 humidity. Therefore, the accumulation profile of humidity measured at $(\text{H}_2\text{O})_2 \text{H}^+$, M_{37} , was the most
235 distinct breath-driven profile. The visual inspection of the shape of VOC profiles led to a sample of 24
236 masses which showed an accumulation profile similar to the profile of humidity. Examples are depicted in
237 (cp. Fig. 2a–d). This led to the assumption that a similarity in shape indicated their origin from breath. To
238 systematically identify these VOCs, a HCA was applied to the accumulation profiles of all recorded
239 masses. Noteworthy, the clustering tree started at the lowest level with the mass of humidity M_{37} (Fig. 2e).
240 The members of this cluster tree branch resembled the VOCs with the most similar profiles to the pattern
241 of humidity (e.g., M_{41} , M_{45} , M_{61}).



243

244 **Fig. 2** Selection of similar VOCs profiles and section of the cluster tree of a hierarchical cluster analysis
 245 (HCA) applied to the accumulation profiles. a Humidity, detected as protonized water clusters $\text{H}_2\text{O}\cdot\text{H}_3\text{O}^+$
 246 (M_{37}) is the most prominent constituent in exhaled breath. By visual inspection, b M_{41} (fragment of
 247 propanol), c M_{45} (acetaldehyde/ CO_2), and d acetic acid (M_{61}) show very similar profiles. The relative
 248 uncertainty in the derived concentration in ppb due to the uncertainty in the measured count rate estimated
 249 to 10 % or less. Note that the error bars due to the counting statistics were still about the size of the
 250 symbols in Fig. 2b, e.g., the profile with a low concentration. e Section of the cluster tree obtained when
 251 the HCA is applied to the matrix of profiles of 120 masses of a PTR-MS analysis. Remarkably, the
 252 clustering starts with the humidity masses M_{37} and M_{39} without any supposition. The branch includes the
 253 masses with the most similar profiles to that of the humidity profile

254

255 Sensing environmental confounders

256 Routinely, four accumulation profiles were recorded in a sequence with every mouse. First, a baseline
 257 measurement of the clean, empty box was screened for leakage and contaminations. Then, three
 258 accumulation profiles in succession were recorded with a mouse. Within a sequence of profiles, the
 259 incidence of confounders resulted in distortions of the profiles, e.g., mice released small amounts of urine

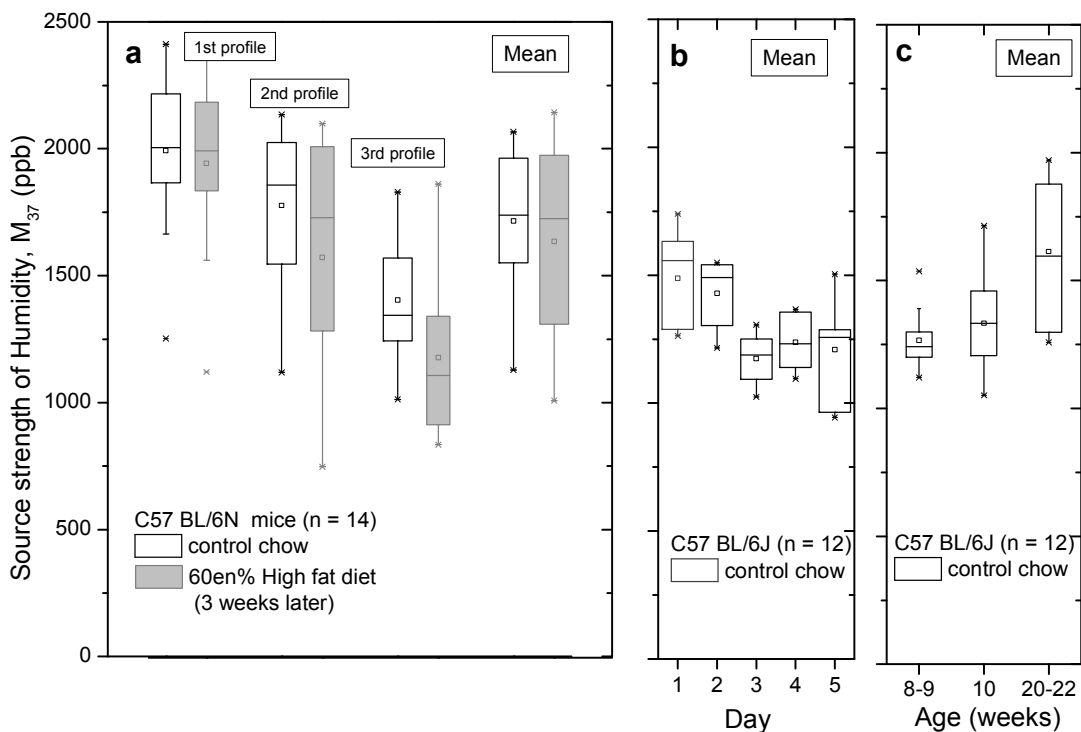
260 and feces into the respirometry chamber during accumulation profiling which polluted the gas
261 compartment (head space) in the chamber. Detailed head space analysis of these confounders with PTR-
262 MS had shown disturbing effects interfering with exhaled VOCs. A unique urine and feces marker at
263 M_{49} (tentatively assigned to methanethiol) could be detected, which remained at a low level of 0.1 ppb but
264 immediately crossed this threshold concentration in presence of small urine droplets in the chamber. In
265 addition, a droplet of urine added an additional source of humidity, and therefore, clearly increased the
266 concentration of humidity. Based on these observations, profiles of VOCs were regarded as undisturbed
267 and selected for further analysis when the concentration of M_{49} was below 0.1 ppb. Training and adapting
268 of the mouse to the respirometry chamber before the measurement considerably reduced the
269 contamination rates due to urine or feces to roughly to one in four cases.

270 **Variability of accumulation profiles**

271 The repeatability of the measured accumulation profiles were analyzed in short- (subsequent profiles),
272 medium-(day-by-day), and long-term (weeks) investigations. The three sequenced accumulation profiles
273 recorded from a mouse revealed a frequent variation (cp. Fig. 2a). The saturation levels of profiles of
274 humidity recorded one after another and therefore the source strength S_{M37} often decreased. By observing
275 the behavior of the mouse during the profile measurement variation could be related to behavioral
276 patterns, in which an initially active mouse settled down from profile to profile. In a sample of 14 male
277 C57 BL/6N mice, the median of S_{M37} of a settled mouse (3rd profile) is roughly 30 % lower than that of
278 an active mouse (1st profile) (Fig. 3a). To evaluate the link between activity and source strength of
279 humidity, we simultaneously measured the respiration frequency in a plethysmograph and the profile of
280 VOCs with the PTR-MS connected to this chamber exemplarily in two male C57 BL/6N mice. The
281 derived source strength increased with respiratory frequency ($11.3 \pm 2.9 \text{ ppm ml min}^{-1}$ per 100
282 breathS_{Mi}^{-1}) and clustered at low and higher respiration frequencies. The day-by-day repeatability of the
283 source strength was investigated in a sample of 12 male C57 BL/6J mice (mean weight $27.7 \pm 1 \text{ g}$). The
284 mean source strength of humidity was roughly 15 % lower at day 3–5 compared with day 1 and 2 (Fig.
285 3b). Again, day-by-day variation in the source strength of humidity could be related to behavioral patterns
286 especially locomotor activity of the mouse in the respirometry chamber, e.g., a more settled-down
287 behavior at day 3–5 compared to the first 2 days. In a long-term investigation, we repeatedly determined
288 the source strength of VOCs in a sample of 12 male C57BL/6J mice with an age of 8–9 weeks (mean
289 body mass: $25.6 \pm 2.3 \text{ g}$), 10 weeks (mean body mass: $25.9 \pm 2.2 \text{ g}$), and 20–22 weeks (mean body mass:
290 $31.1 \pm 3.4 \text{ g}$), c.p. Fig. 3c. With increasing age and increasing body mass, the source strength of humidity
291 shifted to a higher mean and broadened (weeks 8–9: 1,241 [99] ppm ml min^{-1} , week 10: 1,315 [209] ppm
292 ml min^{-1} , weeks 20–22: 1,590 [450], ppm ml min^{-1} , values in brackets denote the Q3–Q1 interquartile

293 range). We observed a relation between humidity source strength and body mass following an
 294 allometrical mass scaling exponent of 0.69 ± 0.17 (Lighton 2008) that is typically found also for the
 295 relation of energy turnover and body mass. The difference in humidity may be related to the age-related
 296 increase in body mass and may be seen as a general read-out for body mass-dependent increase in energy
 297 expenditure.

298

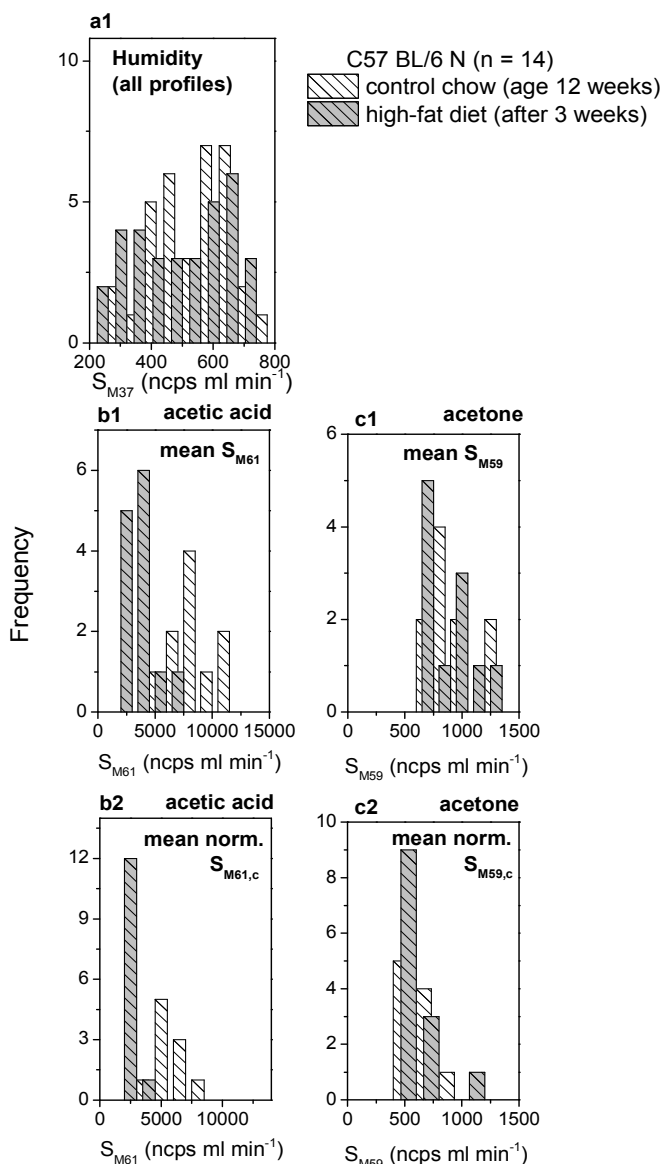


299
 300 **Fig. 3** The repeatability of the measured accumulation profiles in short- (subsequent profiles), medium-
 301 (day-by-day), and long-term investigations. a Source strength S_{M37} in a sample of 14 male C57 BL/6N fed
 302 with control chow (age 12 weeks, mean body weight 32 ± 3 g) and after a HFD (age 15 weeks, mean
 303 body weight 40.8 ± 3.8 g). As a rule, the 1st profile belonged to an active, and the 3rd profile to a settled
 304 down mouse. b The day-by-day repeatability of the mean source strength S_{M37} in a sample of 12 male C57
 305 BL/6J mice (mean body weight 27.7 ± 1 g). c Long-term investigation of the mean source strength S_{M37} in
 306 a sample of 12 male C57 BL/6J mice: age of 8–9 weeks (25.6 ± 2.3 g), 10 weeks (25.9 ± 2.2 g), and 20–
 307 22 weeks (31.1 ± 3.4 g). The mean body mass is given in parentheses

308

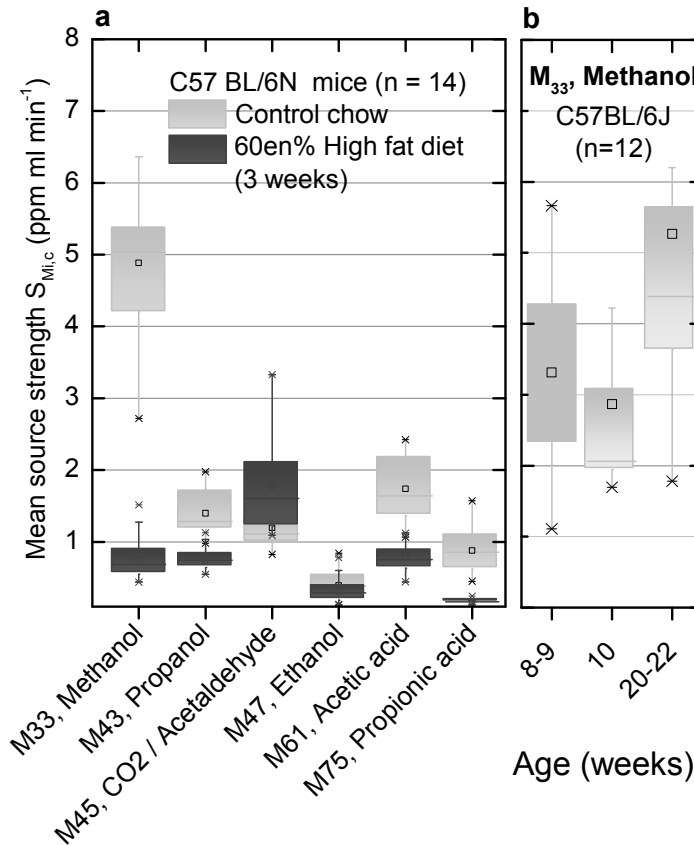
309 **Significant changes in the source strength in response to a dietary intervention**

310 Our main interest was whether a dietary intervention, i.e., feeding a HFD resulted in a statistically
311 significant shift in the source strength of exhaled VOCs. The source strength of 24 breath-driven VOCs
312 was determined in a sample of 14 mice before and after feeding a purified HFD (60 % of the energy from
313 fat). The mean body mass of the C57BL/6N mice initially fed with a control chow diet increased from 32
314 ± 3 g to 40.6 ± 3.8 g within three weeks of HFD. After HFD challenge, the S_{M37} again depended on
315 behavioral characteristics (i.e., calming down) during the measurement of the subsequent accumulation
316 profiles (Fig. 3a) as could be shown before. Evaluating the frequency distribution of S_{M37} from all
317 humidity profiles suggested a bimodal shape (Fig. 4a). This bimodal distribution reflects the observation
318 that mice showed rather high levels of locomotor activity just after the transfer into the chamber, but
319 calmed down when it was kept for a longer time in the chamber. Therefore, S_{M37} can be regarded as a
320 monitor of locomotor activity, whereas other VOCs were clearly influenced by HFD. Irrespective of the
321 behavioral link, e.g., S_{M61} showed distinctly lower levels after feeding the HFD compared with initial
322 levels (Fig. 4b1), whereas other VOCs, e.g., S_{M59} , did not (Fig. 4c1). The obvious changes due to varying
323 levels of locomotor behavior should be accounted for before comparing the derived source strengths of
324 exhaled VOCs. In a first approach, we decided to normalize source strengths to the mean source strength
325 $S_{M37,c} = 300$ ncps ml min^{-1} of obese mice at rest. Hence, with $S_{M37} / S_{M37,c}$, a correction factor was derived,
326 and the S_{Mi} values of the other breath-driven VOCs were corrected, i.e., $S_{Mi,c}$. The distribution of the
327 corrected $S_{M61,c}$ and $S_{M59,c}$ are depicted in Fig. 4b2–c2. Again, $S_{M61,c}$ showed distinctly lower levels after
328 HFD compared with initial levels, whereas $S_{M59,c}$ did not. Several breath-driven VOCs showed distinctly
329 lower levels after HFD compared with initial levels when fed with the control chow, especially M_{33}
330 (methanol), M_{43} (propanol), M_{61} (acetic acid), and M_{75} (propionic acid) (Fig. 5a). The tentatively mass-to-
331 substance assignment is given in parentheses. In the sample of 12 male C57 BL/6J mice S_{M33} of
332 methanol—the substance showing strongest effects of HFD—did not show age-related changes (Fig. 5b).
333 The outcomes of the two feed modes of diets, i.e., control chow and HFD, were compared using the
334 Mann-Whitney-test (significance level 0.05, two-tailed). Table 1 summarizes the statistical significance of
335 the separation of the two samples dependent of the derived source strength: the mean source strength S_{Mi}
336 of three accumulation profiles in series, source strength of the (3rd) accumulation profile of the settled
337 mouse $S_{Mi,3}$, and the mean normalized source strength $S_{Mi,c}$. In the case of mean S_{Mi} , a subset of seven
338 masses (M_{33} , M_{43} , M_{45} , M_{47} , M_{61} , M_{75} , and M_{93}) was significantly separated ($P \setminus 0.001$). As a rule, the
339 separation improved if normalized $S_{Mi,c}$ were used. With the $S_{Mi,3}$, the source strength of the last profile in
340 a mouse measurement, the separation was still significant, but with lower P values in comparison with
341 results for the mean S_{Mi} and $S_{Mi,c}$.



342

343 **Fig. 4** Distributions of the source strengths S_{M37} , S_{M61} , and S_{M59} , evaluated from C57 BL/6N mice initially
 344 fed with a control chow and after a three-week HFD. a1 The bimodal distributions of S_{M37} reflect the
 345 observation that just after its transfer into the box, an active mouse comes to rest with the increasing
 346 residence time in the box. In addition, the histogram of the source strength of obese mice shows a shift
 347 to lower source strengths. b1, c1 The HFD reduced significantly the source strength of acetic acid, S_{M61}
 348 but not of acetone, S_{M59} . b2, c2 The normalized $S_{M_{i,c}}$ to obese mice at rest as a reference. Ncps denotes
 349 the count rate normalized to count rate of the precursor ion and the water cluster at M_{37} according to
 350 (10) (c.p. see "PTR-MS" section)



351

352 **Fig. 5** Change in the corrected source strength $S_{Mi,c}$ of selected VOCs exhaled by C57 BL/6N mice
 353 subjected to a diet challenge and long-term variability of methanol in C57 BL/6J mice fed with control
 354 chow. a The source strength $S_{Mi,c}$ of selected VOCs in the exhaled breath of 14 male C57 BL/6N mice
 355 shift significantly to smaller values after a 3-week-long feeding up with 60 energy% HFD. In the case of
 356 methanol, S_{M33} decreased down to 10 % of the initial value of chow-fed mice. The boxes show the
 357 medians, Q1 and Q3, and the symbols denote 5 and 95 percentiles. b In a control group of C57 BL/6J
 358 mice, the exhaled methanol level did not drop when fed with the control chow for more than 10 weeks

359

360 **Table 1** Statistical significance of the separation of the source strength distributions of two samples of
 361 mice fed the control chow and HFD in dependency of the derived source strength

362 Outcome of the two feedings were tested using the Mann-Whitney Test (significance level 0.05, two-
 363 tailed) using (1) mean source strength S_{Mi} ($n_1 = 10, n_2 = 13$), (2) source strength of the 3rd profile $S_{Mi,3}$
 364 ($n_1 = 11, n_2 = 10$) and (3) the normalized $S_{Mi,c}$ ($n_1 = 10, n_2 = 13$) to obese mice at rest as a reference

365 threshold. The sample size of mice is noted in parentheses and the masses (substances) whose
 366 distributions of the two groups differed significantly ($P < 0.001$) were shaded.

Protonated mass number, MH^+	Substance (tentatively assigned)	P-value		
		mean S_{Mi}	$S_{Mi,3}$	mean $S_{Mi,c}$
M_{31}		0.059	0.42	0.4
M_{33}	methanol	$6.3 \cdot 10^{-5}$	$1.2 \cdot 10^{-4}$	$6.3 \cdot 10^{-5}$
M_{37}	water cluster	0.78	0.098	1
M_{41}		$2.4 \cdot 10^{-3}$	0.038	$3.2 \cdot 10^{-3}$
M_{43}	propanol fragment	$3.6 \cdot 10^{-4}$	$3.2 \cdot 10^{-4}$	$6.3 \cdot 10^{-5}$
M_{45}	CO ₂ /acetaldehyde	$6.3 \cdot 10^{-5}$	$1.2 \cdot 10^{-4}$	$3.2 \cdot 10^{-3}$
M_{47}	ethanol	$3.8 \cdot 10^{-4}$	0.045	0.18
M_{59}	acetone	0.31	0.062	0.44
M_{61}	acetic acid	$1.06 \cdot 10^{-4}$	0.062	$6.3 \cdot 10^{-5}$
M_{75}	propionic acid	$6.3 \cdot 10^{-5}$	$1.2 \cdot 10^{-4}$	$6.3 \cdot 10^{-5}$
M_{93}		$7.0 \cdot 10^{-3}$	0.027	0.088

367

368

369 Discussion

370 Methodological aspects

371 We developed a respirometry setup adapted to PTR-MS and suitable for the screening of exhaled VOCs
 372 in the breath of unrestrained laboratory mice. We hypothesized that VOC signatures in exhaled breath
 373 reflect the metabolic status of mice investigated in experimental studies to decipher causes and
 374 pathogenesis of human metabolic disorders. Therefore, the access to this group of substances—VOCs—
 375 previously not addressed by other technologies (approaches such as metabolomics or proteomics, etc.)
 376 may provide valuable additional information regarding dysfunctional metabolic pathways related to
 377 disease. Here, we report results of initial feasibility studies evaluating the practicability, robustness, and
 378 usefulness of VOC breath gas analysis in mice. Contrary to directly sampling the breath gas via intubation
 379 or specifically adapted mouthpieces, our setup is based on head space measurements of unrestrained mice
 380 making use of the accumulation of VOCs in a respirometry cage. While implementing this setup, it cannot
 381 be ruled out that VOCs do not only originate from the blood stream being exchanged and exhaled via the
 382 lung. Therefore, we aimed to specify which other sources of VOCs may confound the analysis and which

383 sources of variability in VOCs can be identified. Mouse urine contains a considerable number of VOCs,
384 which are unique to this species, and some of them strongly depend on sex and endocrine status
385 (Schwende et al. 1986). With PTR-MS, the signal at, tentatively assigned to methanethiol, was identified
386 as a unique monitor for urine and feces. This signal was at low levels of around 0.1 ppb if the mouse in
387 the respirometry chamber did not urinate or defecate. By controlling this sensitive and immediate monitor
388 marker, VOC profiles that did not satisfy specific criteria like smoothness of the profile and concentration
389 of a marker below a threshold value were rigorously excluded. The evaporation rate of VOCs from urine
390 varies with the urine sources (i.e., droplet size, spots and wet fur), and this does not allow an estimation of
391 the contribution to the concentration in the headspace. In this feasibility study, the link of particular
392 masses to chemical substances was not evaluated by means of other methods (e.g., GC-MS). However, in
393 PTR-MS, a correlation plot of isotopes of a compound may support a tentative assignment of the
394 compound behind a mass. The assignment of methanethiol to M_{49} was supported by the finding that the
395 concentration of M_{51} corresponded with 5 % of the count rate of M_{49} roughly to the second-most abundant
396 isotope of methanethiol, M_{51} . During the measurement of the accumulation profiles, a mouse is likely to
397 vary in physical activity levels. After being transferred to the respirometry chamber, the mouse exhibited
398 exploratory behavior and grooming, but it settles down after habituation. Such changes in physical
399 activity levels resulted in variation of the minute volume of exhaled breath. Lung mechanics is profoundly
400 affected by breathing frequency (Bates and Irvin 2003). Reinhard et al. (2002) reported a great diversity
401 between inbred mice strains, including the C57BL/6J strain, for lung function parameters. Among other
402 differences, the total lung capacity and the pulmonary diffusing capacity for carbon monoxide varied by
403 50 % and the static lung compliance by a factor of 2 between the strains. On the other hand, there was no
404 simple allometric relationship of lung size with body mass. These results were based on defined
405 respiratory maneuvers in anesthetized mice. In our unrestrained plethysmography test in conscious S_{Mi} ce,
406 the changing of physical activity resulted in a decrease in S_{M37} by roughly 30 % when the mouse settled
407 down. The normalization to a VOC which relates to a reference behavioral state, e.g., the source strength
408 of humidity of a settled mouse, may improve the statistical significance of the difference in the source
409 strengths of exhaled VOCs due to a nutrition challenge. However, the impact of this normalization on the
410 distribution of S_{Mi} has to be carefully reviewed in order not to distort the dependence on other
411 physiological parameter. The measuring set-up was intended to analyze the headspace under conditions
412 which do not massively induce stress in mice. The mice were handled with great care and adapted to the
413 chamber before breath gas analysis. Increased activity, urination and defecation are early visible markers
414 for stress. By definition, measurements with urine and feces contamination were discarded. Still, we
415 found a fluctuation of the sources strength of 30 % during habituation in this study, which may partly be
416 related to stress. Published data on GC-analysis of the headspace of urine showed that mouse urinary

417 biomarkers provided, among others, signature typical for stress (Schaefer et al. 2010). Therefore, a careful
418 evaluation of changes in the CO₂ and humidity source strength in combination with a PTR-MS search for
419 stress biomarkers evaporating from urine should be addressed to further refine the method.

420 Short-term changes in physical activity level during the accumulation of a profile modulate the shape of
421 the VOC profiles. Therefore, the assumption of constant source strengths had to be refined by an extended
422 respirometry chamber model with a source strength which takes into account sudden changes. When
423 exemplarily applied to a selection of smooth and modulated profiles, the additional time dependent term
424 had only marginal effects on the fit but essentially improved the fit in disturbed, modulated profiles. As a
425 consequence, the whole profile need not be discarded because the undisturbed part of the accumulation
426 profile can be used. In PTR-MS, breath gas is not being processed prior to analysis. The quantitative
427 determination of the concentration of some VOCs at dry and low CO₂ condition just after the flushing of
428 the respirometry chamber with dry synthetic air may differ from the humid and CO₂-enriched conditions
429 after a few minutes of exhalation (Keck et al. 2008; Schwarz et al. 2009). The count rate of humidity cps
430 (M₃₇) of 0.5–2.5 % of the count rate of the primary ions [cps(M₁₉)] at the end of an accumulation profile
431 was low compared to that of the saturated humidity of (human) breath (cps(M₃₇)/ cps(M₁₉) = 60 %).
432 Nevertheless, the suggested normalization of the measured count rate, which includes the consumption of
433 primaries due to water clusters, was applied (Lindinger et al. 1998). Common VOCs in (human) breath
434 show substantial fragmentation depending on the humidity and CO₂ content (Keck et al. 2008). For
435 selected VOCs, a correction due to this fragmentation should be considered in future.

436 **Intervention study**

437 Investigations of exhaled VOCs of small animals such as aS_{Mice} were previously restricted to single VOCs
438 such as ethanol. Cope et al. (2000) reported on ethanol production in 20-week-old lean mice. After a 30-
439 min equilibration time in a respirometry chamber, they recorded concentrations of about 10 ppb ml⁻¹ CO₂.
440 If we assume 3 vol% of CO₂ in air, a breathing rate of 130 min⁻¹ at rest, and 0.3 ml tidal volume, the
441 source strength of ethanol can be estimated as 0.26 nl min⁻¹. This is comparable to the source strength of
442 1.8 nl min⁻¹ of a mouse at rest fed with a standard laboratory chow in our pilot study, especially if taking
443 into account that the ethanol production underlies a daily rhythm (Cope et al. 2000). In this feasibility
444 study, we applied breath gas analysis for metabolic profiling in mice initially fed with a standard
445 laboratory chow diet and then a HFD containing 60 energy% of fat. We identified a set of VOCs that were
446 significantly reduced after the HFD intervention of three weeks, especially the source strength of
447 methanol. In recent years, the importance of mammalian gut microbiota on the metabolism of their host
448 organism has been widely acknowledged. A possible correlation between microbiota metabolism and

449 obesity is under discussion (Cani and Delzenne 2009; Tilg and Kaser 2011; Vrieze et al. 2010). Aprea et
450 al. (2012) reported that the methanol concentration in the breath of rats fed with a HFD which was half of
451 the concentration when fed with a standard diet. These authors suggested that the difference can be
452 related to the digestion of fibers by the gut microflora; however, the link to microbial activity was only
453 rarely addressed experimentally. Future nutrition challenge experiments have to be carefully designed to
454 distinguish between matrix characteristics and the fat composition of the diets. Acetic acid (M_{61}) and
455 propionic acid (M_{75}) are important endogenously produced and circulated metabolites in mice. As their
456 abundance was reduced in the breath after HFD, we hypothesize that these compounds were utilized for
457 gluconeogenesis in the liver (propionic acid) or as substrate for the synthesis of cholesterol and lipids in
458 the peripheral tissues (acetic acid) (Samuel et al. 2008). However, alcohols and short chain fatty acids
459 (SCFA), such as acetic acid and propionic acids, are products of gut bacteria, too. These metabolites can
460 be easily absorbed from the colon into the blood and may influence carbohydrate and lipid metabolism
461 and thus may profoundly interact with the metabolism of the mouse.

462 **Conclusion**

463 In conclusion, we could show that online breath gas analysis by PTR-MS can be adapted to the
464 dimensions of a mouse regarding the small exhaled minute volume. Further progress will be enabled by
465 the recently implemented commercial PTR-TOF-MS in the breath gas screen which records full mass
466 spectra within a second. In combination with higher mass resolution, extended mass range, and higher
467 sensitivity in mass range above $m/z * 100$ compared to the PTR-MS with a quadrupole mass analyzer, the
468 refinement of the compartment model, and the development of a multiplexed set-up, become feasible
469 thereby increasing study capacities in a high throughput phenotyping screen such as the GMC.

470 In our feasibility study, despite the intra-individual variability in the source strength induced by
471 behavioral characteristics of an unrestrained mouse, a set of VOCs was found to be significantly altered in
472 response to the dietary intervention. These VOCs can be related to physiological functions and metabolic
473 pathways and may be useful as markers for metabolic phenotyping. It remains to be clarified whether
474 these changes are related to the metabolism of the mouse, to metabolites originating from gut microbiota,
475 or to an interaction of microbiota metabolites with mouse metabolism. Further studies addressing this
476 aspect are in progress. Animal studies could improve our understanding of the metabolic pathways and
477 correlated breath gas components in mouse models for human disorders. Standardized housing
478 conditions, a defined genetic predisposition to diseases and the possibility to investigate the interaction of
479 lifestyle factors (e.g., nutrition, physical activity) and targeted metabolic alterations in established
480 challenge experiments provide the possibility to decipher subsets of target VOCs in the exhaled breath of

481 mice. A promising perspective is their use and the search for these target VOCs in human breath which
482 may otherwise not be identified as biomarkers in human breath due to the human intra- and inter-
483 individual variability. This has the potential of being clinically useful for the early noninvasive diagnosis
484 of diseases, physiological disorders, and therapeutic monitoring. In this sense, the use of breath tests as a
485 diagnostic tool for human disorders will greatly benefit from animal models.

486 **Acknowledgments**

487 The studies were supported by the grants from the German Federal Ministry of Education and Research
488 (NGFN-Plus, Grant Nos.: 01GS0850, 01GS0869, and Infrafrontier Grant No. 01KX1012). They were
489 also supported by funding from the German Federal Ministry of Education and Research (BMBF) granted
490 to the German Center for Diabetes Research (DZD e.V.).

491

492 **Author contributions**

493 W. S. and J.R. conception and design of methodology.

494 W.S., D.P., S.K., M. Kistler., M. Kneipp and H.S. performed experiments and data evaluation.

495 W.S., J.R. and V.H. interpreted results of experiments.

496 W.S. and J. R. drafted manuscript.

497 M. Klingenspor, C.H. and M.H.A. edited manuscript.

498 **References**

499 Aprea E, Morisco F, Biasioli F, Vitaglione P, Cappellin L, Soukoulis C, Lembo V, Gasperi F, D'Argenio
500 G, Fogliano V, Caporaso N (2012) Analysis of breath by proton transfer reaction time of flight mass
501 spectrometry in rats with steatohepatitis induced by high-fat diet. *J Mass Spectrom* 47:1098–1103

502 Bajtarevic A, Ager C, Pienz M, Klieber M, Schwarz K, Ligor M, Ligor T, Filipiak W, Denz H, Fiegl M,
503 Hilbe W, Weiss W, Lukas P, Jamnig H, Hackl M, Haidenberger A, Buszewski B, Miekisch W, Schubert
504 J, Amann A (2009) Noninvasive detection of lung cancer by analysis of exhaled breath. *BMC Cancer*
505 9:348

506 Bates JHT, Irvin C (2003) Measuring lung function in mice: the phenotyping uncertainty principle. *J Appl*
507 *Physiol* 94:1297–1306

508 Cani PD, Delzenne NM (2009) Interplay between obesity and associated metabolic disorders: new
509 insights into the gut microbiota. *Curr Opin Pharmacol* 9:737–743

510 Cao W, Duan Y (2007) Current status of methods and techniques for breath analysis. *Crit Rev Anal Chem*
511 37:3–13

512 Cope K, Risby T, Diehl AM (2000) Increased gastrointestinal ethanol production in obese mice:
513 implications for fatty liver disease pathogenesis. *Gastroenterology* 119:1340–1347

514 Drorbaugh JE, Fenn WO (1955) A barometric method for measuring ventilation in newborn infants.
515 *Pediatrics* 16:81–87

516 Friedrich M, Petzke KJ, Raederstorff D, Wolfram S, Klaus S (2011) Acute effects of epigallocatechin
517 gallate from green tea on oxidation and tissue incorporation of dietary lipids in mice fed a high-fat diet.
518 *Int J Obes* 36(5):735–743

519 Fuchs H, Gailus-Durner V, Adler T, Pimentel JA, Becker L, Bolle I, Brielmeier M, Calzada-Wack J,
520 Dalke C, Ehrhardt N, Fasnacht N, Ferwagner B, Frischmann U, Hans W, Holter SM, Holzlwimmer G,
521 Horsch M, Javaheri A, Kallnik M, Kling E, Lengger C, Maier H, Mossbrugger I, Morth C, Naton B, Noth
522 U, Pasche B, Prehn C, Przemec G, Puk O, Racz I, Rathkolb B, Rozman J, Schable K, Schreiner R,
523 Schrewe A, Sina C, Steinkamp R, Thiele F, Willershauser M, Zeh R, Adamski J, Busch DH, Beckers J,
524 Behrendt H, Daniel H, Esposito I, Favor J, Graw J, Heldmaier G, Hofler H, Ivandic B, Katus H,
525 Klingenspor M, Klopstock T, Lengeling A, Mempel M, Muller W, Neschen S, Ollert M, Quintanilla-
526 Martinez L, Rosenstiel P, Schmidt J, Schreiber S, Schughart K, Schulz H, Wolf E, Wurst W, Zimmer A,
527 Hrabe de Angelis M (2009) The German Mouse Clinic: a platform for systemic phenotype analysis of
528 mouse models. *Curr Pharm Biotechnol* 10:236–243

529 Hansel A, Jordan A, Warneke C, Holzinger R, Lindinger W (1998) Improved detection limit of the
530 proton-transfer reaction mass spectrometer: on-line monitoring of volatile organic compounds at mixing
531 ratios of a few pptv. *Rapid Commun Mass Spectrom* 12:871–875

532 Hrabe de Angelis M, Strievens M (2001) Large-scale production of mouse phenotype: the search for
533 animal models for inherited diseases in humans. *Brief Bioinformatics* 2:170–180

534 Isken F, Klaus S, Petzke KJ, Loddenkemper C, Pfeiffer AFH, Weickert MO (2010) Impairment of fat
535 oxidation under high-vs. low glycemic index diet occurs before the development of an obese phenotype.
536 *Am J Physiol Endocrinol Metab* 298:E287–E295

537 Jordan A, Haidacher S, Hanel G, Hartungen E, Mark L, Seehauser H, Schottkowsky R, Sulzer P, Mark
538 TD (2009) A high resolution and high sensitivity proton-transfer-reaction time-of-flight mass
539 spectrometer (PTR-TOF-MS). *Int J Mass Spectrom* 286:122–128

540 Keck L, Hoeschen C, Oeh U (2008) Effects of carbon dioxide in breath gas on proton transfer reaction-
541 mass spectrometry (PTR-MS) measurements. *Int J Mass Spectrom* 270:156–165

542 Lindinger W, Hansel A, Jordan A (1998) On-line monitoring of volatile organic compounds at pptv levels
543 by means of proton-transfer-reaction mass spectrometry (PTR-MS) medical applications, food control and
544 environmental research. *Int J Mass Spectrom Ion Process* 173:191–241

545 Miekisch W, Schubert JK, Noeldge-Schomburg GFE (2004) Diagnostic potential of breath analysis—
546 focus on volatile organic compounds. *Clin Chim Acta* 347:25–39

547 Nicklas W, Baneux P, Boot R, Decelle T, Deeny AA, Fumanelli M, Illgen-Wilcke B, Monitoring FWGH
548 (2002) Recommendations for the health monitoring of rodent and rabbit colonies in breeding and
549 experimental units. *Lab Anim* 36:20–42

550 Phillips M, Gleeson K, Hughes JMB, Greenberg J, Cataneo RN, Baker L, McVay WP (1999a) Volatile
551 organic compounds in breath as markers of lung cancer: a cross sectional study. *Lancet* 353:1930–1933

552 Phillips M, Herrera J, Krishnan S, Zainb M, Greenberg J, Cataneo RN (1999b) Variation in volatile
553 organic compounds in the breath of normal humans. *J Chromatogr* 729:75–88

554 Reinhard C, Eder G, Fuchs H, Ziesenis A, Heyder J, Schulz H (2002) Inbred strain variation in lung
555 function. *Mamm Genome* 13:429–437

556 Riely CA, Cohen G, Lieberman M (1974) Ethane Evolution: a new index of lipid peroxidation. *Science*
557 183:208–210

558 Risby TH, Jiang L, Stoll S, Ingram D, Spangler E, Heim J, Cutler R, Roth GS, Rifkind JM (1999) Breath
559 ethane as a marker of reactive oxygen species during manipulation of diet and oxygen tension in rats. *J*
560 *Appl Physiol* 86:617–622

561 Samuel BS, Shaito A, Motoike T, Rey FE, Backhed F, Manchester JK, Hammer RE, Williams SC,
562 Crowley J, Yanagisawa M, Gordon JI (2008) Effects of the gut microbiota on host adiposity are
563 modulated by the short-chain fatty-acid binding G protein-coupled receptor, Gpr41. *PNAS* 105:16767–
564 16772

565 Schaefer ML, Wongravee K, Holmboe ME, Heinrich NM, Dixon SJ, Zeskind JE, Kulaga HM, Brereton
566 RG, Reed RR, Trevejo JM (2010) Mouse urinary biomarkers provide signatures of maturation, diet, stress
567 level, and diurnal rhythm. *Chem Senses* 35:459–471

568 Schwarz K, Filipiak W, Amann A (2009) Determining concentration patterns of volatile compounds in
569 exhaled breath by PTR-MS. *J Breath Res* 3:027002

570 Schwende FJ, Wiesler D, Jorgenson JW, Carmack M, Novotny M (1986) Urinary volatile constituents of
571 the house mouse, *Mus musculus*, and their endocrine dependency. *J Chem Ecol* 12:277–296

572 Smith D, Turner C, Spanel P (2007) Volatile metabolites in the exhaled breath of healthy volunteers: their
573 levels and distributions. *J Breath Res* 1:014004

574 Tilg H, Kaser A (2011) Gut microbiome, obesity, and metabolic dysfunction. *J Clin Investig* 121:2126–
575 2132

576 Vautz W, Nolte J, Bufe A, Baumbach JJ, Peters M (2010) Analyses of mouse breath with ion mobility
577 spectrometry: a feasibility study. *J Appl Physiol* 108:697–704

578 Vrieze A, Holleman F, Serlie MJ, Ackermans MT, Dallinga-Thie GM, Groen AK, van Nood E,
579 Bartelsman JFW, Oozeer R, Zoetendal E, de Vos WM, Hoekstra JBL, Nieuwdorp M (2010) Metabolic
580 effects of transplanting gut microbiota from lean donors to subjects with metabolic syndrome.
581 *Diabetologia* 53:S44

582 Whittle CL, Fakharzadeh S, Eades J, Preti G (2007) Human breath odors and their use in diagnosis. *Ann*
583 *N Y Acad Sci* 1098:252–266

584